Theoretical Investigation of the Cyclic Peptide System Cyclo[(d-Ala-Glu-d-Ala-Gln)m=1-4]

ARTICLE *in* THE JOURNAL OF PHYSICAL CHEMISTRY B · DECEMBER 1997

Impact Factor: 3.3 · DOI: 10.1021/jp9722317

3 AUTHORS:

James P Lewis
West Virginia University
90 PUBLICATIONS **2,790** CITATIONS
SEE PROFILE

Norma H Pawley
Los Alamos National Laboratory
18 PUBLICATIONS **336** CITATIONS
SEE PROFILE

Otto F Sankey
Arizona State University
320 PUBLICATIONS **11,683** CITATIONS
SEE PROFILE

Theoretical Investigation of the Cyclic Peptide System Cyclo[(D-Ala-Glu-D-Ala-Gln)$_{m=1-4}$]

James P. Lewis,*,†,§ Norma H. Pawley,‡ and Otto F. Sankey†

Department of Physics and Astronomy, Arizona State University, Tempe, Arizona 85287-1504, Department of Physics, School of Mines, Golden, CO, and Department of Biochemistry and Biophysics, University of North Carolina, Chapel Hill, North Carolina 27599-7260

Received: July 9, 1997; In Final Form: September 17, 1997[⊗]

Using newly developed theoretical methods, we present preliminary results for some calculated properties of the cyclic peptide system cyclo[(D-Ala-Glu-D-Ala-Gln)$_{m=1-4}$]. These calculations are motivated by the fact that the cyclo[(D-Ala-Glu-D-Ala-Gln)$_2$] cyclic peptide structure was the first cyclic peptide structure synthesized by an experimental group through a self-assembly process. In this paper, we calculate the electronic structure and vibrational mode properties of the isolated ring structures for cyclo[(D-Ala-Glu-D-Ala-Gln)$_{m=1-4}$] and of the cyclic peptide nanotube system cyclo[(D-Ala-Glu-D-Ala-Gln)$_2$]. The HOMO−LUMO gap is wide (∼5.0 eV) yielding a transparent material with possibly unique bioelectronic device applications. In addition, we find that the C−O carbonyl stretch modes and the N−H amide-I stretch modes of these isolated ring structures to be highly localized at around 1773 and 3192 cm^{-1}, respectively.

I. Introduction

Early experimental work had shown that polypeptides (amino acids connected together through peptide groups) could be formed by alternating the chirality of amino acids. One of the earliest examples of this was optical measurements,[1] supported by NMR results.[2] These experiments concluded that regular alternating poly(γ-benzyl D,L-glutamate) mainly assumes a stable left-handed α-helical conformational structure. Furthermore, theoretical investigations revealed that α-helical conformations of L,D copolypeptides possess conformational energies comparable to that of poly(L-peptides) and less than that of other structures (L,D ribbon and L,D helix), as previously proposed.[3] Inspired by these results, a theoretical model was developed proposing the possibility of forming β-type rings stacked parallel or antiparallel and stabilized by van der Waals and hydrogen-bonding interactions.[4] These β-type conformational structures form channels which can be used for transporting ions.

Further research succeeded in synthesizing a variety of polypeptide channels in the β-helical conformation, built by alternating D and L residues. In addition, naturally occurring antiparallel β-helical polypeptide chains, such as Gramicidin A, were discovered and successfully crystallized—its structure indicating a propensity to allow transport of water or potassium ions. More recently, Ghadiri et al. discovered that controlled acidification of alkaline peptide solutions triggered the spontaneous self-assembly of amino acids with a flat ring-shaped confirmation called cyclic peptides made up of an even number of alternating D- and L-amino acid residues.[5] All amide backbone functionalities reside approximately perpendicular to the plane of the ring structure; hence, the peptide side chains lie on the outside of the ensemble thereby creating a hollow core structure. The rings stack together through hydrogen-bonding interactions to form a cylindrical structure with nanoscale dimensions, referred to as nanotubes. Hundreds of these nanotube structures are tightly packed to form crystalline fibers. It was also shown that it is energetically favorable for these ring-shaped cyclic peptides to self-assemble in the lipid bilayer environment, creating a transmembrane channel structure. An eight-residue cyclic peptide, cyclo [(Trp-D-Leu)$_3$ Gln-D-Leu], which has alternating L-tryptophan and D-leucine side chain moieties with the exception of one L-glutamine residue that was introduced mainly to simplify the peptide synthesis, was shown to be three times faster in transporting ions than Gramicidin A under similar conditions.[6] As transmembrane channels, these nanotube structures could be potential vehicles for drug delivery into living cells and may find use in antisense and gene therapy applications.

Through different self-assembly synthesis processes or choice of amino acid chain functionalities employed, a wide range of tubular structures with specified internal diameters and surface characteristics are designed, yielding a wide range of applications. Other than transmembrane channel structures, many possible applications have been proposed for the use of these nanotubes, as discussed in the following examples. First, such tubular materials could be designed to make nanoscale test tubes for studying the physical and chemical properties of inorganic and metallic clusters, having important applications in catalysis and inclusion chemistry. Second, these nanotubes could be designed to mimic pore structures useful in zeolite and clay chemistry. Third, the uses of these nanotubes go well beyond biological or chemical uses, but can also have applications in molecular electronics. These nanotubes can be designed as novel optical and electronic devices or as templates for circuit miniaturization.[5−7]

Given the wide range of applications, it would be of scientific value to investigate several microscopic properties of these cyclic peptide nanotubes, including the energetics, geometrical configurations, and electronic structures. Calculating and understanding these properties would assist in determining the compatibility that certain tubes might exhibit for the previously mentioned applications. For example, the electronic structure and charge densities would assist in understanding the molecular electronics applicability of a studied cyclic peptide nanotube system. Very little theoretical work has been done to study such microscopic properties of these cyclic peptide systems. While the energetics, geometrical structures, and vibrational modes can be studied using empirical methods, a study of these systems using quantum mechanical methods has been performed to obtain a more complete picture of their properties such as

† Arizona State University.
‡ School of Mines.
§ University of North Carolina.
⊗ Abstract published in *Advance ACS Abstracts,* November 15, 1997.

S1089-5647(97)02231-1 CCC: $14.00

the electronic structure. Such information can only be theoretically obtained via electronic structure methods. In addition, we have recently developed theoretical methods for the purposes of performing simulations on large biomolecular systems, and as a further confirmation of the method, we examine some calculated properties of these cyclic peptide systems.

In this paper, a preliminary discussion is presented for some properties of a few cyclic peptide systems, using newly developed theoretical methods. In particular, the structure cyclo-[(D-Ala-Glu-D-Ala-Gln)$_{m=1-4}$] has been studied the most. This is motivated by the fact that the cyclo[(D-Ala-Glu-D-Ala-Gln)$_2$] cyclic peptide structure was the first structure synthesized by Ghadiri et al.[6] The results presented in the next sections cover the energetics, electronic structures and vibrational properties of the isolated ring structures. Although the structures of these isolated monomer are difficult to observe experimentally, it is interesting to investigate the properties of such structures and compare the results to their respective nanotube counterparts. Specifically, results of the vibrational spectrum of the cyclo-[(D-Ala-Glu-D-Ala-Gln)$_2$] cyclic peptide nanotube and comparisons with the vibrational spectrum of corresponding isolated ring are presented in this paper. Also in this paper, a preliminary discussion is given on the results of placing a glucose molecule in the cyclo[(D-Ala-Glu-D-Ala-Gln)$_2$] nanotube structure. Before presenting the results, the next section briefly discusses the quantum mechanical methods employed for the calculations of these systems.

II. Computational Methods

By the combination of several recently developed theoretical techniques, an electronic-structure-based method was developed for the purpose of performing molecular-dynamical simulations of large biomolecular systems. We demonstrated the efficiency of this method by performing calculations of a deoxyribonucleic acid (DNA) double-helix poly(dG)−poly(dC) segment containing 10 base pairs as an earlier initial benchmark and test case of the method.[8] The essence of the method can be summarized in three points: (i) there are two energy scales in the Hamiltonian and each is treated differently: the strong intramolecular interactions are treated within approximate density functional theory (DFT), whereas the weak intermolecular interactions (e.g., hydrogen bonds) are described within a simple theory that accounts for Coulombic, exchange, and hopping interactions between the weakly interacting fragments; (ii) a localized basis of atomic states is used, yielding a sparse Hamiltonian and overlap matrices; (iii) the total energies and forces from the sparse Hamiltonian and overlap matrices are solved using a linear scaling technique, which avoids the N^3-scaling problem of standard electronic structure methods.

Many biological systems, such β-sheets, consist of two or more weakly interacting fragments where within each fragment strong intramolecular interactions are present. To describe both the weak and strong interaction energy scales simultaneously with sufficient accuracy, we conveniently characterize the total energy in terms of a sum of strong intramolecular and weak intermolecular components. This allows the use of two different models of calculation, where each model is appropriately formulated for each type of interaction. For two weakly interacting fragments, we write the total energy as

$$\langle H_{\text{total}} \rangle = \sum_i \langle H(i) \rangle + \partial U_N^{\text{binding}} \qquad (1)$$

The first term, involving $\langle H(i) \rangle$, is the sum of the total energies over all N noninteracting molecules, and the second term, $\partial U_N^{\text{binding}}$, represents the intermolecular interaction between the N molecules. The intramolecular interactions are relatively large in energy (on the order of 1000 eV for an amino acid unit), but the intermolecular interaction is quite small compared to these intramolecular terms (on the order of 0.25 eV or 5 kcal/mol for a hydrogen bond) and changes more readily according to the geometry of the system.

The intramolecular interactions are determined from a first principles local orbital method developed by Sankey and Niklewski.[9] This is done using the Harris functional within the local density approximation (LDA), and using the pseudopotential approximation.[10,11] The electronic eigenstates are expanded as a linear combination of pseudo-atomic orbitals within a localized sp^3 basis for carbon, nitrogen, and oxygen, as well as s-basis for hydrogen. This method has been applied to many covalent systems and has proven to be computationally fast and quantitatively accurate.[12]

To calculate weak intermolecular interactions such as in hydrogen-bonded systems, we use a method that was previously developed and discussed for the case of interacting H_2O dimers and trimers.[13] This method was shown to work well for a large H_2O system containing 216 molecules and for isolated DNA base pairs and triplets.[14,15] In calculating the intermolecular interactions, a linear combination of atomic orbitals (LCAO) of the Slater type (STOs) are used, since this is the expected asymptotic shape in the intermolecular regions. The orbitals on each molecule overlap with its neighboring molecules, but since this intermolecular overlap is small, the effects of overlap are Taylor series expanded and are treated only to the second order. The interactions between molecules that we include are electrostatic, exchange, and one-electron "hopping" interactions. The one-electron "hopping" interactions include a repulsive overlap interaction and an attractive rehybridization contribution. Additional attractive interactions between molecules occur due to electrostatic and exchange contributions. Also, van der Waals energies and forces are included empirically via the Slater−Kirkwood approximation, which is based on a weighted average of the dispersion coefficients C_6 due to each individual atoms polarizability and its effective number of electrons.[16]

For large systems, determining the electronic eigenvalue (band structure) energy via matrix diagonalization must be avoided due to the N^3 scaling. A linear in N-scaling technique is the desirable method of choice for determining the band structure energy. In the past few years, a number of methods with linear scaling have been proposed, most of which are applicable provided that the Hamiltonian and overlap matrices of the system are sparse in a localized orbitals basis, which is certainly the case in our formulation for large systems.[17,18] For nonmetallic systems, the occupied electron orbitals can be constructed to be exponentially localized Wannier-like states. Beyond some (small) cutoff range R_c, the overlap and Hamiltonian interactions between these Wannier-like occupied orbitals can be neglected.[19] In the method we use here, an energy functional is formulated which takes advantage of the sparse Hamiltonian and overlap matrices for the system under consideration. The electronic ground state of the system is obtained by minimizing the energy functional with respect to all possible localized states, which are expanded in terms of the atomic orbital basis (only those entering the localization sphere of radius R_c are included in this expansion). The advantage of this energy functional is the fact that no orthogonality constraints need to be imposed during the minimization, since the form of the functional drives the wave functions toward orthogonalization. In other words, the minimum is achieved for orthogonal functions and for the exact ground-state band energy.[18]

The energy functional is minimized iteratively using the method of conjugate gradients.[20] In this method, a succession of line minimizations is performed, where the minimization directions are given by the "force-like" gradient of the energy functional, corrected to make the successive directions orthogonal to each of the former iterations. The "forces" of the energy functional are just the derivatives of the energy functional with respect to the coefficients of the expansion of the occupied orbitals in terms of the basis functions. This procedure is repeated until the value of the energy functional is minimized and unchanged within some tolerance. All the computations involved (gradients and energy functional) scale linearly with the number of electrons, as long as the occupied states are localized within a radius R_c. This technique avoids the $O(N^3)$ complexity involved in the orthogonalization process present in standard iterative minimization procedures, as well as in matrix diagonalization. We refer the reader to ref 18 for the details of the order-N method used in this work.

Forces for each atom at position $\vec{r}_i$ are determined by taking the analytic derivative of the energy with respect to $\vec{r}_i$, where the derivative of the electronic term is determined on the basis of the Hellmann−Feynman theorem.[21] A sixth-order interpolation algorithm obtains the derivatives of the electron single-particle Hamiltonian matrix elements, which exactly includes Pulay corrections,[22] from the precalculated integral data tables. All calculations, throughout this paper, are performed on a IBM RISC 6000 workstation. From the resulting forces, molecular dynamics simulations can be carried out by solving the equations of motion using the Gear predictor-corrector algorithm.[23] In searching for a minimum energy configuration, a dynamical quenching process is used. In this process the equations of motion are solved and the resulting kinetic energy determined. When the kinetic energy reaches a maximum, the velocities are quenched (set to zero), and the process is repeated until a zero force configuration is obtained.

III. Results of the Cyclo[(D-Ala-Glu-D-Ala-Gln)$_{m=1-4}$] Isolated Ring Structures

In this section, some theoretically determined properties of isolated monomer ring structures of the cyclic peptide systems cyclo[(D-Ala-Glu-D-Ala-Gln)$_{m=1-4}$] are discussed. Figure 1 shows theoretically optimized geometries of these structures. Simulations were performed to determine the energetics, electronic structure, and vibrational spectra of such systems, utilizing the local orbital method with O(N) implementations as previously discussed. These simulations did not include any solvent molecules and conditions resemble the gas phase. In general, the formation of a cyclic peptide ring structure from alternating the chirality of amino acids would appear energetically unfavored; however, because the rings may stack together through hydrogen bonding interactions, their stability is greatly increased.[24] Even though these ring structures have not been isolated experimentally, it is interesting to investigate these systems as a basis for the larger nanotube system.

The energy per atom versus the ring size of the isolated ring structures cyclo[(D-Ala-Glu-D-Ala-Gln)$_{m=1-4}$] was calculated, and the results are presented in Figure 2. The results indicate that the energy for $m = 1$ is considerably higher than the energies for $m = 2-4$. From Figure 1 it appears that there is a large backbone strain on the isolated ring structure cyclo[(D-Ala-Glu-D-Ala-Gln)$_1$], compared to the other structures. Experimentally it is noted that cyclic D,L- peptides of less than six residues have too small of an internal diameter, and because of this prohibitively large backbone strain, the peptide backbone will not adopt the required geometry for intermolecular hydrogen-bonding stacking interactions. Furthermore, such small diameter ring structures are not useful in the context of nanotube designs.[26]

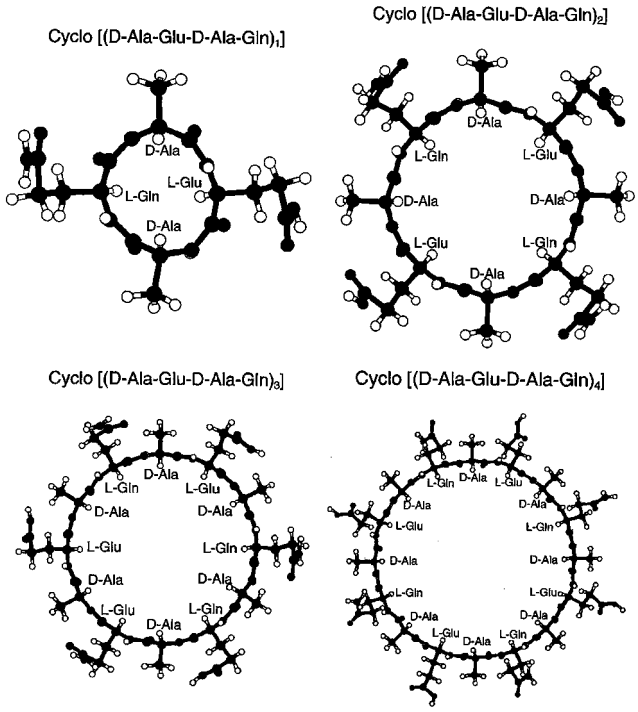

Figure 1. Geometries of the isolated ring structures cyclo[(D-Ala-Glu-D-Ala-Gln)$_{m=1-4}$]. The structures shown are the final structures obtained from a molecular dynamics relaxation.

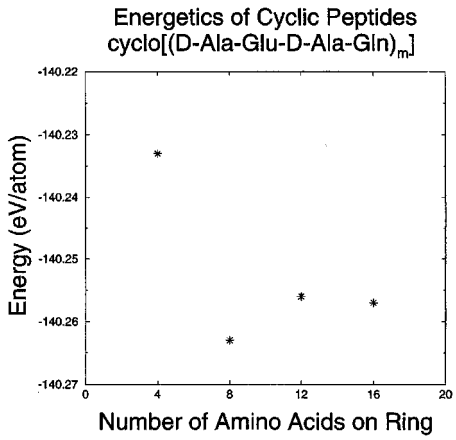

Figure 2. Energy of the isolated monomer ring structure cyclo[(D-Ala-Glu-D-Ala-Gln)$_{m=1-4}$] versus the number of amino acids in the ring. The energy for $m = 1$ is much higher than the remaining structures, but for $m = 2-4$ the energies are all within kT_0 ($T_0 = 300$ K) of each other.

The results of Figure 2 also demonstrate that the energetics of the isolated ring structure for $m = 2-4$ are within kT_0 ($T_0 = 300$ K) of each other. This suggests that diameters of almost any radius can be synthesized without penalty. Entropic effects however must also be considered, which likely limit the diameter of the nanotubes. This is supported experimentally, since it is reported that due to the greater flexibility of the peptide backbone, too large of a ring structure will not sample in the flat ring-shaped conformational state to effectively take part in the nanotube self-assembly process.[26] Both theoretical and experimental results confirm that the range of nanotube diameters is confined between 7 and 13 Å.

The electronic density of states for the isolated ring structure cyclo[(D-Ala-Glu-D-Ala-Gln)$_{m=1-4}$] are present in Figure 3. The energy gap values, measured as the difference between the

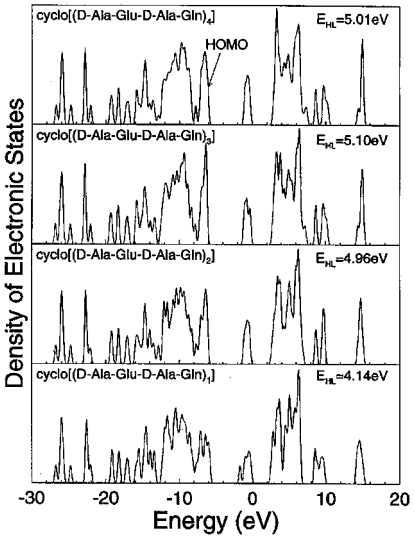

Figure 3. Calculated electronic density of states (DOS) for the isolated monomer ring structures cyclo[(D-Ala-Glu-D-Ala-Gln)$_{m=1-4}$]. In general, all the electronic DOS contain very similar features.

highest occupied molecular orbital (HOMO) and the lowest unoccupied molecular orbit (LUMO), are indicative of most proteins, which are largely transparent. The values that are obtained for the energy gaps are approximately 5.0 eV, except for the smallest ring. The smallest ring gives an energy gap value of 4.14 eV, and the energy gap is reduced due to dispersion of the energy levels from the small diameter of the ring, implying that one side of the ring interacts strongly with the other side of the ring. The fact that these materials have large gaps is supported experimentally by Ghadiri et al. who reported that colorless prismatic crystals are obtained.[25]

A few other interesting points can be mentioned about the electronic structures results of Figure 3. As seen in Figure 3, the electronic structure of the isolated ring structures shows very localized states at ~ -26 and ~ -23 eV corresponding to the oxygen and nitrogen 2s-states, respectively. Earlier results of DNA, using our method, did not demonstrate this very localized nature (for example, the width of the nitrogen 2s-states is approximately 1 eV for the cyclic peptides, but the DNA results indicate that the width is between 2−3 eV).[8] The very localized oxygen and nitrogen 2s-states may be a characteristic feature of the cyclic peptide systems. Note that the peptide group, which connects the two amino acids, is formed with a nitrogen−carbon bond made up of residues with alternating chirality. The localized nature of the nitrogen electronic 2s-state perhaps suggests that the bonds formed in these peptide groups have little sp-hybridization characteristics compared to other covalent interactions in the ring structure. The bond may be weaker because the alternating chirality of the amino acids may produce a less stable peptide bond in the cyclic peptide compared to the peptide bonds normally found in proteins. As previously discussed, this is also supported experimentally since much of the stability to the nanotubes comes from the hydrogen-bonded stacking network and not from the peptide backbone.[24,25]

One fascinating property of these cyclic peptide nanotubes is that for biological materials they are extremely stable. Recently, Hartgerink et al. report that the cyclic peptide nanotube crystals are stable to highly acidic (pH = 1) and strongly basic solutions (pH = 14) and can even survive boiling water.[26] In addition, they are stable in most common polar and nonpolar organic solvents. With regards to stability, most other biological materials do not even come close. The high stability of these nanotubes makes them an ideal candidate for molecular electronic devices as well as other applications.

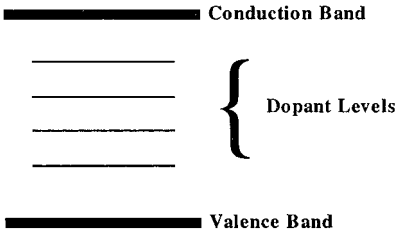

Figure 4. A schematic diagram of a ladder of dopant levels that may occur in a wide bandgap material. This is one of many possible uses for the wide bandgap cyclic peptide systems. These systems would make good microelectronic devices compared to most other biological materials given their great stability under a variety of environmental conditions.

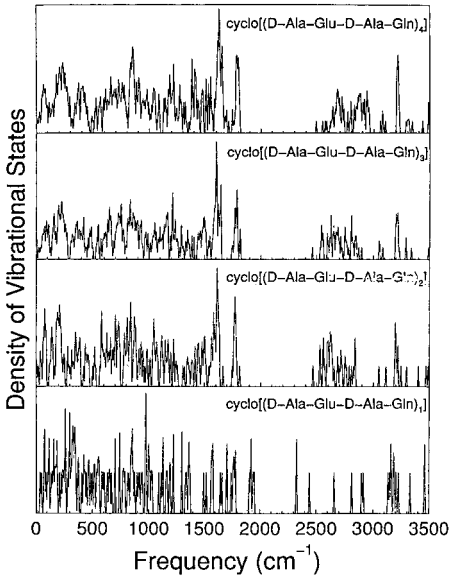

Figure 5. Calculated vibrational density of states for the isolated ring structures cyclo[(D-Ala-Glu-D-Ala-Gln)$_{m=1-4}$]. In general, all the vibrational spectra contain very similar features.

These cyclic peptide systems have bandgaps that are greater than "standard" semiconducting materials. However, the features of an open-ended hollow tubular structure implies that an assortment of materials can be packed inside to obtain a variety of molecular electronic devices. For example, it has been suggested that if one side of the tube is doped p-type and the other doped n-type, then diodes/transistors on the nanoscale dimensions could be designed.[27] The features of a large bandgap imply that a ladder of levels, from the valence bond to the conduction band as shown in Figure 4, can be engineered by choosing appropriate dopant materials. Also, since the bandgap is large, the self-conduction is minimal and the conduction across the device will be mainly through the dopant levels. Finally, the electronic structures of all the isolated ring structures show very similar density of states. This may imply that the effects of a particular dopant may also be independent of the tube diameter, allowing for a greater flexibility in the designed applications.

The calculated vibrational spectra for the isolated ring structure cyclo[(D-Ala-Glu-D-Ala-Gln)$_{m=1-4}$] are present in Figure 5. All vibrational spectra were obtained by a diagonalization of the dynamical matrix which was constructed by finite differences. The resulting eigenvalues are represented by Gaussians centered on each eigenvalue to give the density of states. In this method each atom is displaced, one at a time, in each direction of space by 0.0125 Å. The forces are computed on all atoms, and dividing by the displacement (assuming a harmonic approximation) gives one column of the force constant

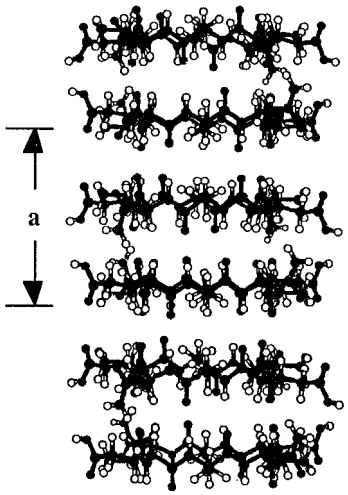

Figure 6. Nanotube constructed from cyclo[(D-Ala-Glu-D-Ala-Gln)$_2$] cyclic peptides. The isolated ring structures stack on top of each other through hydrogen bonding. Hundreds of these nanotube structures (much longer than what is shown) are tightly packed to form crystalline fibers.

matrix. Cubic anharmonic terms are removed by averaging the dynamical matrix using positive and negative displacements.

A comparison of the vibrational spectra indicates that they are all qualitatively the same. A simlar observation was noted for the electronic density of states. From these vibrational spectra, two groups of highly localized vibrational modes, averaging 1773 and 3192 cm^{-1}, are found. Examination of the eigenvectors indicates that the first group of localized modes corresponds to a stretch mode of the C−O bonds, while the second group corresponds to a stretch mode of the N−H bonds. Both set of bonds lie perpendicular to the cyclic peptide backbone, perhaps explaining the nature of the modes having a localized characteristic. The localized signature of these bonds within these cyclic peptide structures could be important for determining sample purity in the synthesis process which would be necessary in product design. Each behaves similar to a classic picture of an isolated single harmonic oscillator attached to a infinite mass object such as a wall, which is a good comparison to both set of bonds considering that the mass of the extended atom is much less than the remaining peptide ring. Also, it is interesting to note that the C−O stretch mode is similar in frequency to that of a CO molecule ($\nu = 2150$ cm^{-1}), but with a slightly higher mass (which will downshift the frequency).

This completes the discussion of the results for the electronic and vibrational density of states of the isolated ring structures cyclo[(D-Ala-Glu-D-Ala-Gln)$_{m=1-4}$]. Good qualitative agreement exists between these theoretical results and those of experiment. In the next section, results for nanotube structures will be discussed. In particular, the discussions of the next section will concentrate on the cyclic peptide system cyclo[(D-Ala-Glu-D-Ala-Gln)$_2$] and comparisons will be made to the corresponding isolated ring structures.

IV. Results of Cyclic Peptide Nanotubes

The isolated ring structures, as shown in Figure 1, will stack through an extensive network of hydrogen-bonding to form cylindrical hollow tubes of nanoscale dimensions. An example of one such nanotube for the cyclic peptide sequence cyclo-[(D-Ala-Glu-D-Ala-Gln)$_2$] is shown in Figure 6. Hundreds of these nanotube structures [much longer than what is shown in Figure 6] are tightly packed to form crystalline fibers. The crystal structure for cyclo[(D-Ala-Glu-D-Ala-Gln)$_2$] nanotube system is experimentally determined to have a triclinic unit cell.[5] This low-symmetry crystal structure is due to the fact that the ring structures have only C_2 symmetry. For a series of other cyclic peptide sequences with C_4 symmetry, (cyclo[(Gln-D-Ala)$_4$] cyclo[(Gln-D-Val)$_4$], cyclo[(Gln-D-Leu)$_4$], cyclo[(Gln-D-Phe)$_4$]), the crystal structure was experimentally determined to slightly deviate from a tetragonal unit cell, which has higher symmetry than the triclinic unit cell. Theoretical investigations of these higher symmetry cyclic peptide systems will be the discussion of future work.

For the cyclo[(D-Ala-Glu-D-Ala-Gln)$_2$] cyclic peptide nanotube structure, energy minimizations were performed to determine the theoretical lattice parameters and compare these results with experiment. In these calculations, the energy was calculated for several values of the lattice parameter, a and c. No solvent molecules were added in the simulation, and conditions resemble a solid cystalline state, the crystal structure of which can be viewed in Figure 3 of ref 5. We theoretically determined the lattice parameter to be $a = 10.78$ Å and $c = 16.13$ Å, where experimentally the values are determined to be $a = 9.5$ Å and $c = 15.1$ Å. Our theoretical results are consistently about 10% over that of the experimental values, which is the same degree of accuracy obtained for our results of water and DNA base molecules.[13,15] For the minimum energy configuration obtained, we calculate the binding energy per dimer to be 58.65 kcal/mol. This compares favorably to experimental work, where it is determined that each hydrogen-bond will contribute 4.0−5.6 kcal/mol, depending on the solvent employed, yielding between 64.0 and 89.6 kcal/mol additional binding energy of the nanotube over the isolated ring structure for the cyclic peptide system cyclo[(D-Ala-Glu-D-Ala-Gln)$_2$].[24,25]

In addition, note that there are two arrangments for the isolated ring structures of cyclo[(D-Ala-Glu-D-Ala-Gln)$_2$] to be stacked. Along the tube's axis, either identical (Glu-Glu-Glu, etc.) or alternating (Glu-Gln-Glu, etc.) side chain functionalities can be stacked adjacent to each other. The lattice parameters previously presented are for the case where the side chain functionalities alternate. For the case where the side chain functionalities are identical, the calculated lattice parameters only slightly increased and the energy of this structure is determined to be only slightly higher (0.002 eV/atom $\ll kT_0$) than for the case where the side chain functionalities are alternate. Experimentally, there is yet no observation of which side chain functionality pattern exists, but theoretically they are energetically equivalent.

Vibrational spectra for both the isolated ring structure and the nanotube structure of the cylic peptide sequence cyclo[(D-Ala-Glu-D-Ala-Gln)$_2$] is shown in Figure 7. The highly localized frequencies of the C−O stretch mode shift from an average of 1773 cm^{-1} to an average of 2073 cm^{-1} and the N−H stretch modes shift upward from an average of 3192 cm^{-1} to an average of 3387 cm^{-1}. Infrared absorption experiments of cyclo[(D-Ala-Glu-D-Ala-Gln)$_2$] cylic peptide nanotube structure reports a frequency of 3277 cm^{-1} for the N−H stretch mode and a range of frequencies between 1628 and 1736 cm^{-1} with large peaks at 1628 and 1688 cm^{-1}.[5]

A comparison of experimental results for the C−O stretch mode with the theoretical results, shown in Figure 7, indicates that the theoretical trends are correct. In both cases the amide-I mode *increases* as a result of the hydrogen-bonding interactions between the ring structures in the nanotube. In the experimental results, the increase is about 50 cm^{-1}, whereas the theoretical results indicate a 300 cm^{-1} increase. Since the C−O stretch mode increases more significantly compared to the N−H stretch mode in the presence of hydrogen bonding, it is evident that

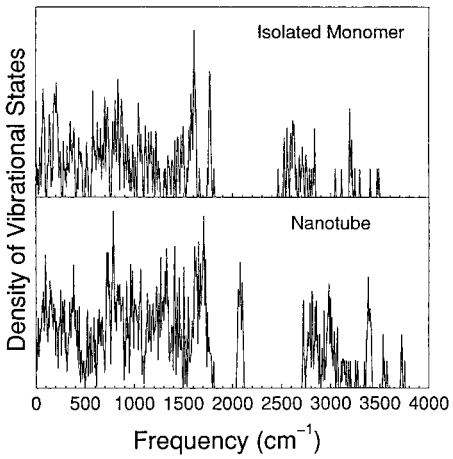

Figure 7. Vibrational spectra of the cylic peptide sequence cyclo[(D-Ala-Glu-D-Ala-Gln)$_2$] for both the isolated ring structure and the nanotube structure. The highly localized vibrational modes corresponding to the C−O stretch mode and the N−H stretch mode have shifted to higher frequencies.

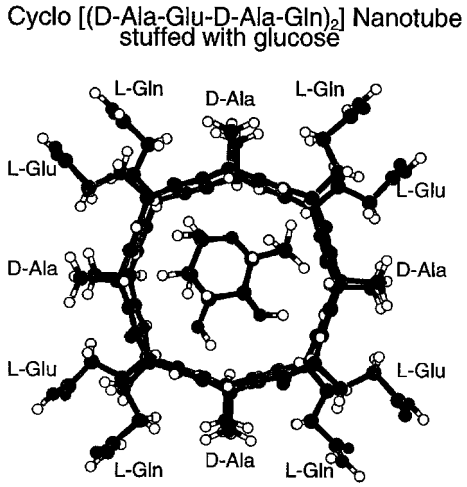

Figure 8. Geometry of the cyclic peptide structure cyclo[(D-Ala-Glu-D-Ala-Gln)$_4$] nanotube stuffed with a glucose molecule. This is a view looking down the tube axis. Results of a simulation indicate that the diameter of this nanotube is too small to allow transport for the glucose molecule.

the large theoretical error is mostly due to the pseudopotentials used in modeling oxygen atoms, yielding too strong a hydrogen-bonding interaction. Other experimental evidence supports that in certain configurations of hydrogen bonding, such as an antiparallel-chain rippled sheet polyglycine I structure, the stretching mode frequency will indeed actually increase.[28] These frequency shifts as a result of the hydrogen-bonding interactions between the ring structures in the nanotube may be theoretically understood by a simple spring model (see Appendix).

Further experimental work was done by Granja and Ghadiri to design, synthesize, and characterize the first artificial transmembrane pore structure which displays efficient glucose tranport activity.[6] A specially designed cyclic peptide structure, cyclo[Gln-(D-Leu-Trp)$_4$-D-Leu], was used to self-assemble into a lipid bilayer. This structure contains 10 amino acid residues, has approximately a 10.0 Å diameter, and was demonstrated to be ideal for glucose transport through a lipid bilayer. In contrast, gramicidin A, a naturally occurring ion channel-forming peptide with a 4.5 Å diameter, and the cyclo[Gln-(D-Leu-Trp)$_3$-D-Leu] cyclic peptide structure, which has an internal diameter of 7.5 Å, were shown to yield no glucose transport.

A theoretical investigation was inititated in order to begin to understand the mechanisms behind transport activity through the cyclic peptide systems. As shown in Figure 8, a glucose molecule was placed in the cyclo[(D-Ala-Glu-D-Ala-Gln)$_2$] cylic peptide nanotube in two locations, first located within a ring structure and second between two ring structures. The cyclic peptide nanotube chosen has a 7.5 Å diameter, and although the tube seems large enough, no transport was expected based on the experimental results. This structure was chosen to first understand why the transport of glucose does not occur in this nanotube. For both locations of the glucose molecule, a simulation was performed to minimize the energy of the system. In both cases, the glucose contracted due to "pressure" from the nanotube, while the nanotube did not appear affected by the glucose molecule. The intermolecular binding energy of the glucose was lowest for the case where the molecule was placed inside the ring structure, rather than for the case where the glucose was placed between two ring structures. Another simulation was performed where the glucose was given an initial velocity corresponding to $T = 300$ K. In this simulation, the glucose was quickly bound and trapped within the nanotube, unable to move any further down the tube. The results of these preliminary simulations indicate that the particular chosen nanotube is indeed too small for transport, which is exactly as found in the experimental results of the cyclo[Gln-(D-Leu-Trp)$_3$-D-Leu] cyclic peptide structure.

This section covers only a few results regarding the cyclic peptide nanotubes. There are numerous other theoretical investigations that can be done for other nanotubes and comparisons can be made. For the case of the cyclo[(D-Ala-Glu-D-Ala-Gln)$_2$] cylic peptide nanotube, the results presented here for the vibrational density of states, and in particular the upward shift of the C−O stretch mode, indicate good qualitative agreement with experiment. The lack of glucose transport through this nanotube is also in agreement with similar experimental results.

V. Summary

A new class of materials, formed from amino acids with alternating chirality, was investigated in this paper. As compared to experimental oservations, good qualitative theoretical results for the electronic structure and the vibrational spectra were obtained for the isolated cyclic peptide structures cyclo[(D-Ala-Glu-D-Ala-Gln)$_{m=1-4}$]. In particular, these structures are transparent, as verified by experimental work, and the HOMO−LUMO bandgap for such structures is around 5.0 eV. The nature of the bandgap and the high stability of these biological materials in a variety of pH and temperature conditions suggests that this material can be engineered to yield useful microelectronic devices. Further work will expand upon this feature by studying the effect of the electronic structure due to a variety of dopant materials within the cyclic peptide nanotube. We also note definate isolated N−H stretch modes and C−O stretch modes which may be an important signature for the synthesis process. Comparisons were also made in the vibrational spectra between the isolated ring structures and the nanotubes indicating that the N−H and C−O stretch mode shifts upward due to the hydrogen bonding, as confirmed in experimental work. In addition, preliminary results were reported on the attempts to place glucose within a cyclic peptide nanotube in order to study transport properties. These results will be used as the basis for further work where such properties will be theoretically examined.

Acknowledgment. We greatly appreciate funding through the Office of Naval Research (Grant ONR 00014-90-J-1304)

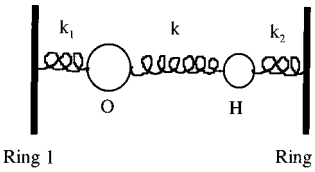

Figure 9. This schematic drawing represents the hydrogen-bonding that takes place between the C−O carbonyl bond of ring 1 and the N−H bond of ring 2. The oxygen and hydrogen atoms are connected to the cyclic peptide rings through strong covalent interactions. These interactions are represented by the harmonic spring constants k_1 and k_2. There is a weak hydrogen-bonding interaction between the oxygen and hydrogen atoms, which is represented by the harmonic spring constant k.

and the National Institute of Health (Grant RR08102-04S1). One of the authors (N.H.P.) thanks the National Science Foundation for the opportunity to participate in the REU program at ASU during which time this research was initiated. We express our appreciation to our colleagues who have generated insightful and stimulating discussion on the topic of this research: Alex Demkov, Tom Drouillard, Matt Grumbach, and Wolfgang Windl. We thank members at the Scripps Research Institute, Reza Ghadiri, Jeff Hartgerink, and Duncan McRee, for all the assistance that they have provided.

Appendix: Simple Spring Model for Describing Amide-I Vibrational Modes in Cyclic Peptide Rings Due to Hydrogen-Bonding Effects

In this Appendix, a simple harmonic spring model is formulated in order to demonstrate that, given the right physical conditions, the carbonyl mode will shift upward in frequency. A model is proposed in Figure 9 where an oxygen atom and a hydrogen atom are attached to two stationary points which represent the cyclic peptide rings. The oxygen and hydrogen atoms bond with the cyclic peptide rings through strong covalent interactions, and are represented by harmonic spring constants k_1 and k_2. There is a weak interaction between the oxygen and the hydrogen atom represented by a spring constant k, where $k \ll k_1, k_2$. It is understood that physically these spring constants will actually decrease as a result of the forming hydrogen bond and that this model is an oversimplification. Experimental evidence showing that the stretch modes increase with the formation of the hydrogen bond perhaps indicates that, in the case of cyclic peptides, the spring constants do not decrease as much as in normal hydrogen-bonding systems.

For the classical harmonic system of Figure 9, the total Hamiltonian is written as

$$H = T + V \tag{A.1}$$

where

$$T = \frac{1}{2}m_1\dot{x}_1^2 + \frac{1}{2}m_2\dot{x}_2^2 \tag{A.2}$$

and

$$V = \frac{1}{2}k_1x_1^2 + \frac{1}{2}k(x_1 - x_2)^2 + \frac{1}{2}k_2x_2^2 \tag{A.3}$$

To obtain the eigenfrequencies of this model, the secular equation

$$\det[\mathbf{V} - \omega^2\mathbf{T}] = 0 \tag{A.4}$$

must be solved, where

$$\mathbf{V} = \begin{bmatrix} \frac{\partial^2 V}{\partial x_1^2} & \frac{\partial^2 V}{\partial x_1 \partial x_2} \\ \frac{\partial^2 V}{\partial x_2 \partial x_1} & \frac{\partial^2 V}{\partial x_2^2} \end{bmatrix} \tag{A.5}$$

and

$$\mathbf{T} = \begin{bmatrix} \frac{\partial^2 T}{\partial \dot{x}_1^2} & \frac{\partial^2 T}{\partial \dot{x}_1 \partial \dot{x}_2} \\ \frac{\partial^2 T}{\partial \dot{x}_2 \partial \dot{x}_1} & \frac{\partial^2 T}{\partial \dot{x}_2^2} \end{bmatrix} \tag{A.6}$$

Upon substitution of $\mathbf{V}$ and $\mathbf{T}$ the secular equation is

$$\det\begin{bmatrix} -m_1\omega^2 + k_1 + k & -k \\ -k & -m_2\omega^2 + k_2 + k \end{bmatrix} = 0 \tag{A.7}$$

having the solution

$$(k_1 + k - m_1\omega^2)(k_2 + k - m_2\omega^2) - k_2 = 0 \tag{A.8}$$

If $k \ll k_1, k_2$, then to a first-order approximation, the eigenfrequencies are

$$\omega_1 = \left(\frac{k_1 + k}{m_1}\right)^{1/2} \tag{A.9}$$

and

$$\omega_2 = \left(\frac{k_2 + k}{m_2}\right)^{1/2}$$

since k^2 is negligible. The solution of the secular equation indicates that, for $k > 0$, both the frequency of the C−O (carbonyl) stretch mode ω_1 and the frequency of the N−H stretch mode ω_2 are shifted higher due to the presence of the hydrogen bond.

It is understood that the spring constants will actually decrease as a result of the hydrogen-bonding formation, and that normally the hydrogen bond will create a downward shift in the stretch mode frequency. However, in the cyclic peptides, this appears to not be the case and there is a slight upward shift in the C−O and N−H stretch mode frequency as verified experimentally. Theoretically, this model could still hold provided that the spring constants were to decrease only slightly, so that the new spring constant, $k_1' + k$ or $k_2' + k$, are still greater than the original spring constants k_1, k_2, then the conclusion would still hold that there would be an upward shift in the frequency.

References and Notes

(1) Heitz, F.; Spach, G. *Macromolecules* **1971**, *4*, 429.
(2) Bovey, F. A.; Ryan, J. J.; Spach, G.; Heitz, F. *Macromolecules* **1971**, *4*, 433.
(3) Hesselin, F. T.; Scherga, H. A. *Macromolecules* **1972**, *5*, 455. Ramachandran, G. N.; Chandrasekharan, R. In *The 2nd American Peptide Symposium*; Cleveland, Ohio, 1970; paper 28.
(4) De Santis, P.; Morosetti, S.; Rizzo, R. *Macromolecules* **1974**, *7*, 52.
(5) Ghadiri, M. R.; Granja, J. R.; Milligan, R. A.; McRee, D. E.; Khazanovich, N. *Nature* **1993**, *366*, 324.
(6) Ghadiri, M. R.; Granja, J. R.; Buehler, L. *Nature* **1994**, *369*, 301.
(7) Whitesides, G. M.; Mathias, J. P.; Seto, C. T. *Science* **1991**, *254*, 1312.
(8) Lewis, J. P.; Ordejón, P.; Sankey, O. F. *Phys. Rev. B* **1997**, *55*, 6880.
(9) Sankey, O. F.; Niklewski, D. J. *Phys. Rev. B* **1989**, *40*, 3979.
(10) Harris, J. *Phys. Rev. B* **1985**, *31*, 1770.

(11) Hamann, D. R.; Schlüter, M.; Chiang, C. *Phys. Rev. Lett*. **1979**, *43*, 1494.

(12) Drabold, D. A.; Ordejón, P.; Dong, J. J.; Martin, R. M. *Solid State Commun*. **1995**, *96*, 833. Demkov, A. A.; Ortega, J.; Sankey, O. F.; Grumbach, M. P. *Phys. Rev. B* **1995**, *52*, 1618.

(13) Ortega, J.; Lewis, J. P.; Sankey, O. F. *Phys. Rev. B* **1994**, *50*, 10516.

(14) Ortega, J.; Lewis, J. P.; Sankey, O. F. *J. Chem. Phys.* **1997**, *106*, 3696.

(15) Lewis, J. P.; Sankey, O. F. *Biophys. J.* **1995**, *69*, 1068.

(16) Halgren, T. A. 1992. *J. Am. Chem. Soc.* **1992**, *114*, 7827.

(17) Yang, W. *Phys. Rev. Lett*. **1991**, *66*, 1438. Drabold, D. A.; Sankey, O. F. *Phys. Rev. Lett*. **1993**, *70*, 3631. Li, X.-P.; Nunes, W.; Vanderbilt, D. *Phys. Rev. B* **1993**, *47*, 10891. Daw, M. S. *Phys. Rev. B* **1993**, *47*, 10895. Stechel, E. B.; Williams, A. R.; Feibelman, P. J. *Phys. Rev. B* **1994**, *49*, 10088. Wang, L.-W. *Phys. Rev. B* **1994**, *19*, 10154. Goedecker, S.; Colombo, L. *Phys. Rev. Lett*. **1994**, *73*, 122. Mauri, F.; Galli, G. *Phys. Rev. B* **1994**, *50*, 4316. Hierse, W.; Stechel, E. B. *Phys. Rev. B* **1994**, *50*, 17811. Hernandez, E.; Gillan, M. J. *Phys. Rev. B* **1995**, *51*, 10157. Ordejón, P.; Artacho, E.; Soler, J. M. *Phys. Rev. B* **1996**, *53*, 10441.

(18) Ordejón, P.; Drabold, D. A.; Grumbach, M. P.; Martin, R. M. *Phys. Rev. B* **1993**, *48*, 14646. Ordejón, P.; Drabold, D. A.; Martin, R. M.; Grumbach, M. P. *Phys. Rev. B* **1995**, *51*, 1456.

(19) Kohn, W. *Phys. Rev.* **1959**, *115*, 809.

(20) Press, W. H.; Flannery, B. P.; Teukolsky, S. A.; Vetterling, W. T. In *Numerical Recipes*; Cambridge: New York, 1986.

(21) Hellmann. H. *Einfuhrung in die Quantumchemic*; Franz Duetsche: Leipzig, 1937. Feynman, R. P. *Phys. Rev.* **1939**, *56*, 340.

(22) Pulay, P. *Theor. Chim. Acta*. **1979**, *50*, 299.

(23) Allen, M. P.; Tildesley, D. J. *Computer Simulation in Liquids*; Oxford: New York, 1987. Gear, C. W. Report ANL 7126; Argonne National Laboratory: Lemont, IL, 1966.

(24) Kobayashi, K.; Granja, J. R.; Ghadiri, M. R. *Angew. Chem., Int. Ed. Engl.* **1995**, *34*, 95.

(25) Ghadiri, M. R.; Kobayashi, K.; Granja, J. R.; Chadha, R. K.; McRee, D. E. *Angew. Chem., Int. Ed. Engl.* **1995**, *34*, 93.

(26) Hartgerink, J. D.; Granja, J. R.; Milligan, R. A.; Ghadiri, M. R. *J. Am. Chem. Soc.* **1996**, *118*, 43.

(27) McRee, D. E. Private communication

(28) Krimm, S.; Bandekar, J. *Adv. Pro. Chem.* **1986**, *38*, 181.